SUPPORTING INFORMATION FILE

Carbon Nanotubes as Electrically Active Nanoreactors for Multi-Step Inorganic Synthesis:

Sequential Transformations of Molecules to Nanoclusters, and Nanoclusters to Nanoribbons

Akos Botos, Johannes Biskupek, Thomas W. Chamberlain, Graham A. Rance, Craig T. Stoppiello, Jeremy Sloan, Zheng Liu, Kazutomo Suenaga, Ute Kaiser, Andrei N. Khlobystov

S1. Details of HRTEM image simulation

Representative image simulations (main article and Supporting Information) were created with the open source SimulaTEM [1s] software using an acceleration voltage of 80 kV, Cs = 0.001 mm and -20 nm defocus. Simulation tableau were generated from rotation arrays of the $[Mo_6I_{14}]^{2-}$ ion produced in the commercial program Crystalmaker.

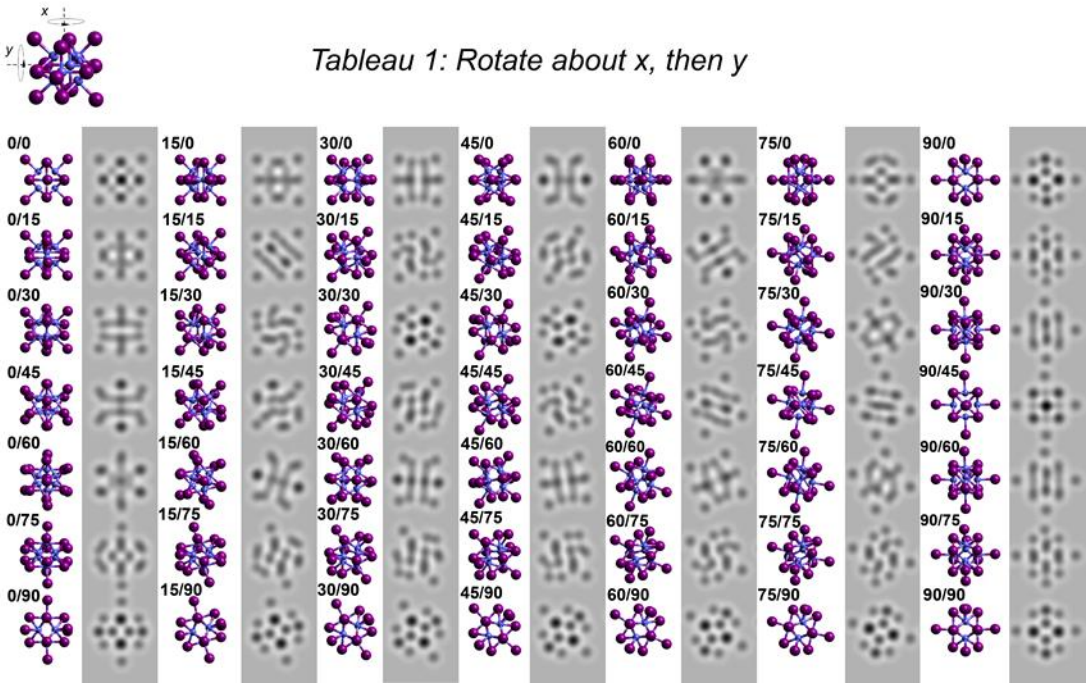

Figure 1s. HRTEM image simulations for $[Mo_6I_{14}]^{2-}$ cluster at 80 keV. Values of the tilt angle are shown in degrees for each orientation.

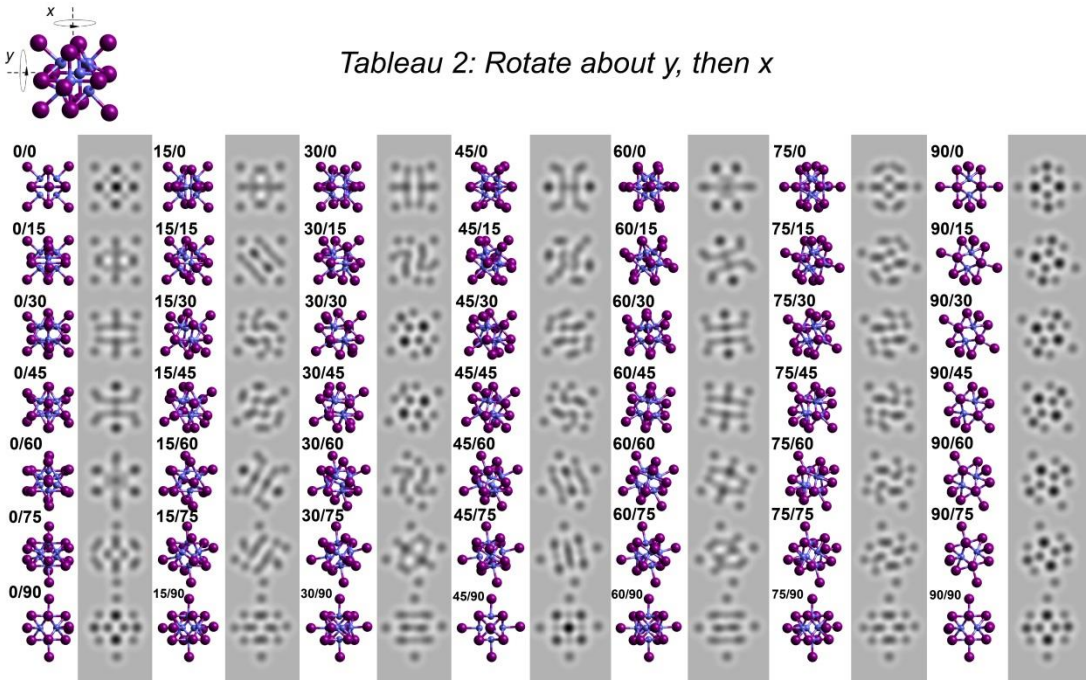

Figure 2s. HRTEM image simulations for $[Mo_6I_{14}]^{2-}$ cluster at 80 keV. Values of the tilt angles are shown in degrees for each projection.

Figure 3s. HRTEM image simulation for aprojection of the cluster along the C_3 rotation axis (equivalent to x/y = 45/0 in the tableau above) of $[Mo_6I_{16}]^{2-}$ in an armchair (11,11) SWNT.

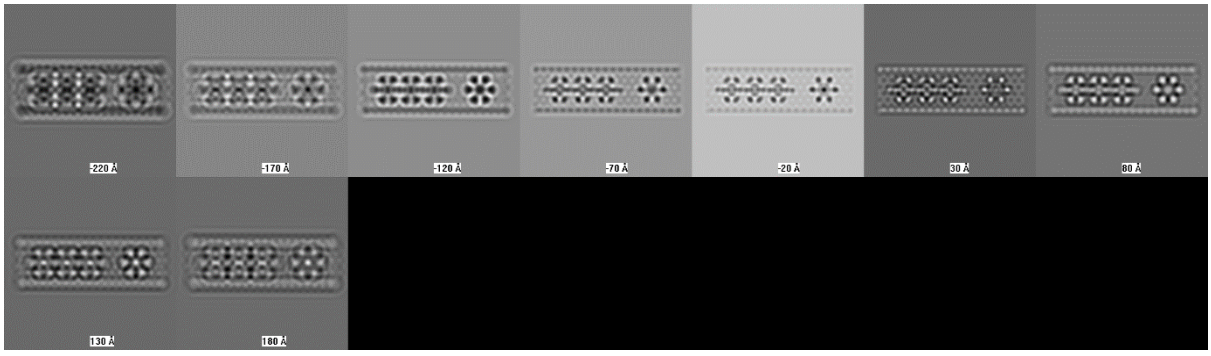

Figure 4s. HRTEM image simulations for a focal series of $[Mo_6I_{12}]_n$@SWNT (Electron energy 80 keV, spherical aberration C_S-= 10 µm, focus spread f_s= 4 nm) ranging from -220 Å to +180 Å in steps 50 Å. Focus of -70Å corresponds to Scherzerfocus.

S2. AC-STEM imaging

Scanning transmission electron microscopy (STEM) annular dark field (ADF) image were taken at 60 kV illustrating the presence of heavy elements inside the nanotube. Metal iodide clusters undergo tumbling motion on the timescale faster than the STEM image capture rate which causes blurring of the nanoclusters, however individual iodine atoms can still be visible on the periphery of some nanoclusters (for example, 5a or 5d). In contrast, metal disulphide nanoribbons (5e) are much more static and therefore STEM imaging is able to reveal atomic positions of W and S.

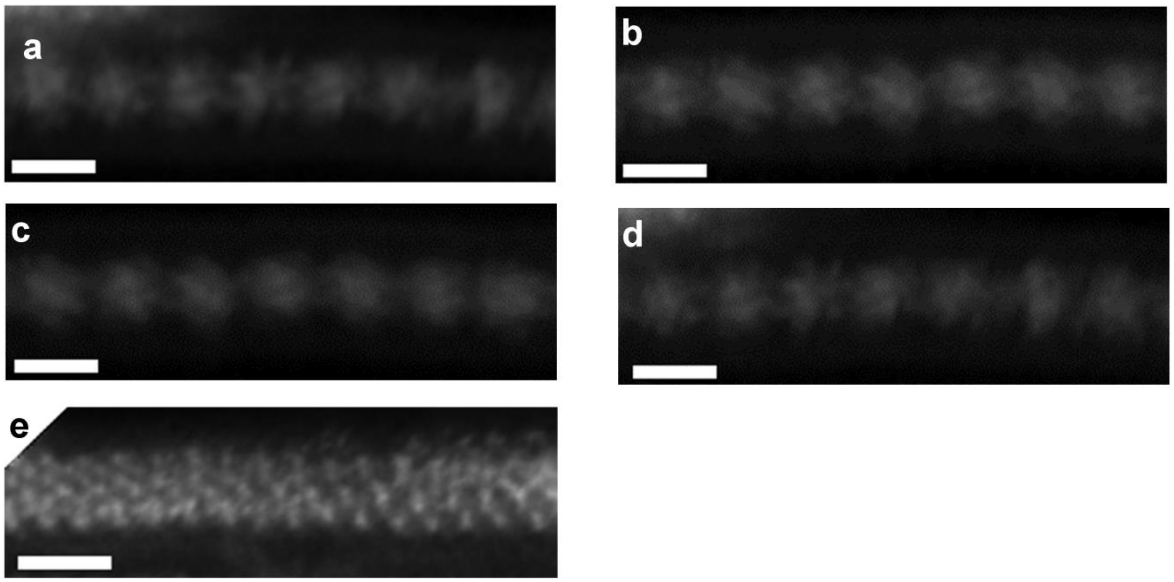

Figure 5s. Scanning transmission electron microscopy (STEM) imaging was performed on a JEOL 2100F with a cold field-emission gun and an aberration DELTA-corrector for the illumination system operated at 60 kV. (a-d) STEM images of $[W_6I_{14}]$@SWNT and (e) $[WS_2]$n@SWNT.

S3. Additional HRTEM and AC-HRTEM images of $[M_6I_{14}]^{2-}$@$SWNT^{2+}$

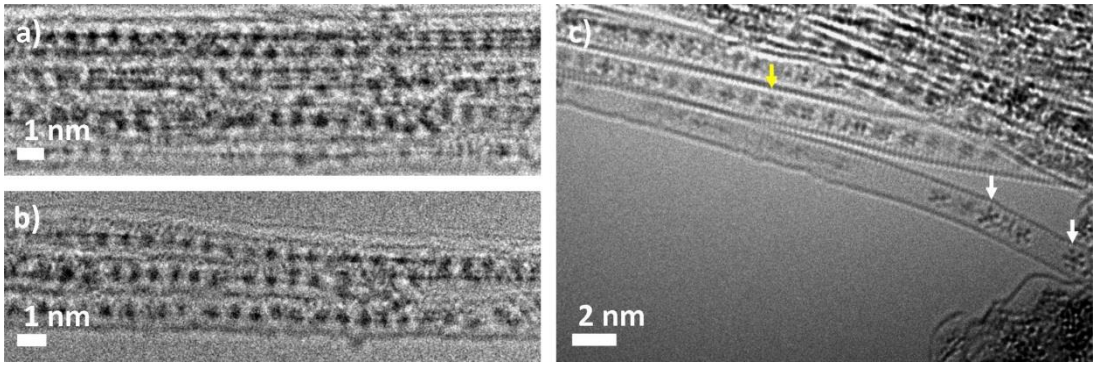

Figure 6s. Low-magnification HERTEM images of W_6I_{14}@SWNTs formed a)-b) dark circular features (*d*=0.7 nm), while c) shows AC-TEM micrographs revealing well-defined geometric shapes, such as star and rhombus, marked with white and yellow arrows.

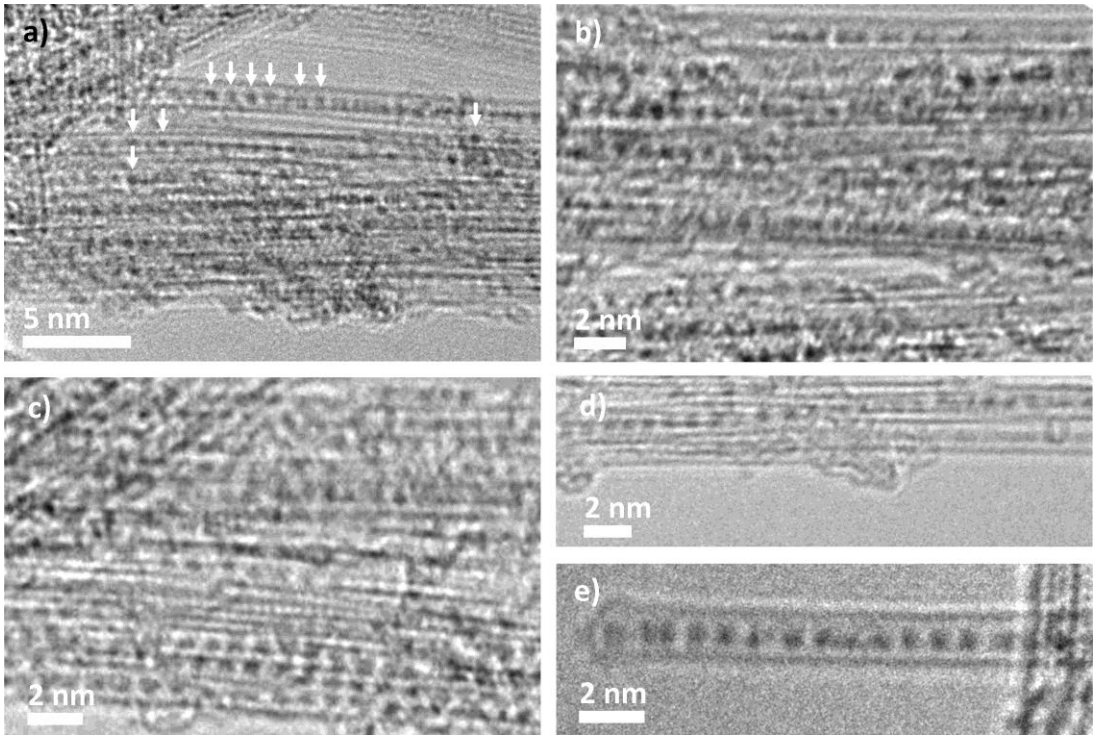

Figure 7s. Low-magnification HRTEM images of Mo_6I_{14}@SWNTs show high-contrast circular features (*d*=0.7 nm) which can be assigned to the molybdenum iodide clusters.

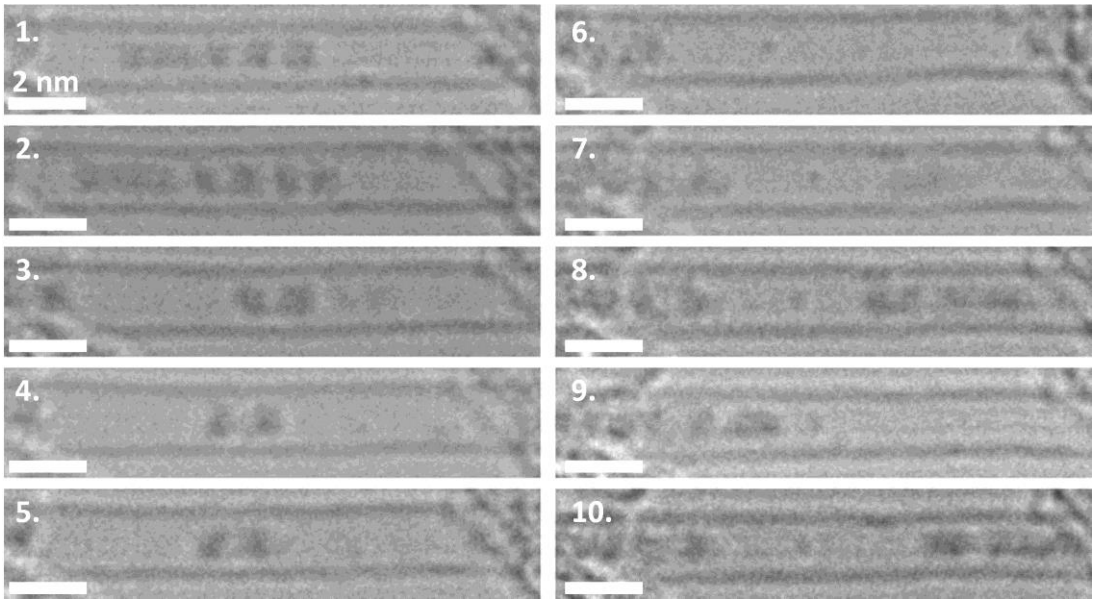

Figure 8s. Time series low-magnification HRTEM images of Mo_6I_{14}@SWNTs shows the movement of high-contrast circular features, corresponding to Mo_6I_{14} clusters, (d=0.7 nm) in SWNTs in MoI_2@SWNTs.

S4. Overall process map of the inorganic synthesis within carbon nanotubes

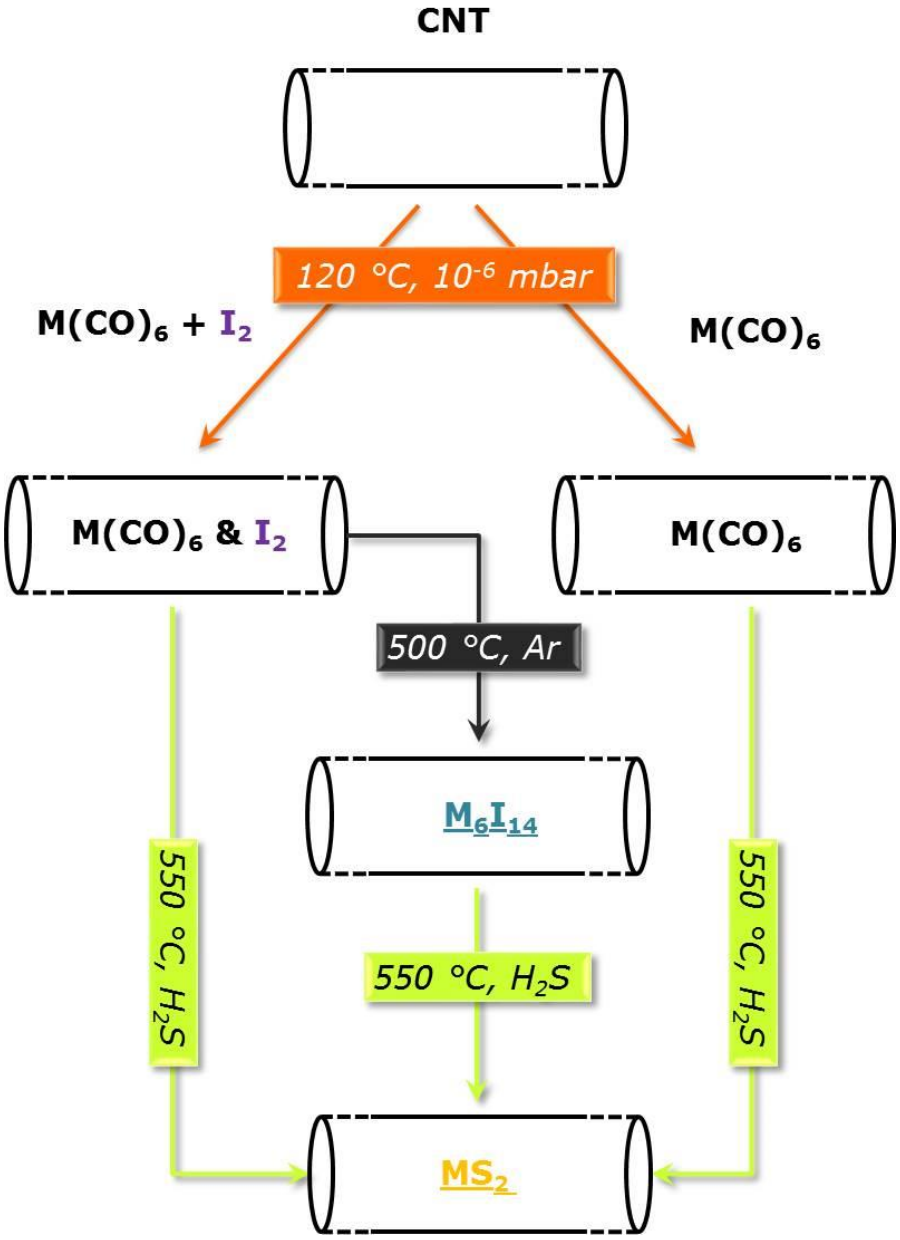

Figure 9s. Schematic diagram summarising the different synthetic strategies utilised to form M_6I_{14}@CNTs and MS_2@CNTs. The orange boxes and arrows represent the encapsulation conditions used to insert precursor molecules into CNTs, while the black box and arrow corresponds to the conversion of $M(CO)_6$ and I_2 precursors inside CNTs and the green boxes and arrows represent the reactions of precursor(s)@CNTs with H_2S.

References

S1. Gómez-Rodríguez, A.; Beltrán-del-Río, L. M.; Herrera-Becerra, R. SimulaTEM: Multislice simulations for general objects, *Ultramicroscopy* **2010**, *110*, 95–104.